

# Correlation and Dimerization Effects on the Physical Behavior of the $NR_4[Ni(dmit)_2]_2$ Charge Transfer Salts : A DMRG Study of the Quarter-Filling $t$ -J Model

Marie-Liesse DOUBLET

*Laboratoire de Structure et Dynamique des Systèmes Moléculaires et Solides USTL II,  
Bât. 15 CC-014, 34095 Montpellier Cédex 5, France*

Marie-Bernadette LEPETIT

*Laboratoire de Physique Quantique, IRSAMC, 118 Route de Narbonne, 31062 Toulouse,  
France  
(May 11, 2018)*

The present work studies the quasi one-dimensional  $Ni(dmit)_2$ -based compounds within a correlated model. More specifically, we focus our attention on the composed influence of the electronic dimerization-factor and the repulsion, on the transport properties and the localization of the electronic density in the ground-state. Those properties are studied through the computation of the charge gaps (difference between the ionization potential and the electro-affinity: IP-EA) and the long- and short-bond orders of an infinite quarter-filled chain within a  $t - J(t, U)$  model. The comparison between the computed gaps and the experimental activation energy of the semiconductor  $NH_2Me_2[Ni(dmit)_2]_2$  allows us to estimate the on-site electronic repulsion of the  $Ni(dmit)_2$  molecule to  $1.16eV$ .

## I. INTRODUCTION

Since the discovery of the Bechgaard salts in the 80's<sup>1</sup>, the interest for such charge transfer *organic* solids is increasing steadily. The molecular character of these systems allows a very large diversity in their structural arrangement as well as in their chemical composition and leads to very rich phase diagrams exhibiting a wide variety of attractive physical properties<sup>2</sup> (charge<sup>3,4</sup> and spin<sup>5</sup> density wave phenomena, electronic<sup>6</sup> or structural<sup>7</sup> localizations, metal to insulator<sup>4,6</sup> or metal to superconductor phases transitions<sup>8</sup>, etc ...). Among the latter, those related to the anisotropy of the conductivity (1D, pseudo-1D or 2D) and hence, to the electronic instabilities of the Fermi surface<sup>9-12</sup> or to the strongly correlated character of the electronic structure<sup>13</sup> receive considerable attention. The physical origin of the conduction band constitutes an important characteristic that classifies the different compounds into :

- one-band 3/4-filled systems for which the conductivity is insured by the Highest Occupied Molecular Orbital (HOMO) of the donors — such as the *TTF*-based molecules<sup>2,14</sup>,
- one-band 1/4-filled systems for which the conductivity is insured by the Lowest Unoccupied Molecular Orbital (LUMO) of the acceptors — such as  $M(dmit)_2$  and related molecules<sup>15</sup>,
- multi-bands systems for which the conductivity is insured both by the HOMO of the donor molecules and the LUMO of the acceptor ones<sup>16</sup>.

These systems have been extensively and fruitfully studied using non correlated models such as tight-binding (one-band model) and extended Hückel (orbital model) methods<sup>17,18</sup> for periodic systems. The topology of the inter-molecular interactions and the occurrence of a nesting vector<sup>12</sup> on the Fermi surface is sufficient to understand the electronic instabilities that induce first order metal to insulator phase transitions<sup>10–12</sup>, such as Charge Density Waves and Peierls distortions<sup>4</sup>. However second order phase transitions, that see the metallic properties being gradually destroyed by electron localization, cannot be explained without the introduction of electronic repulsion<sup>6</sup>. More generally the interaction between the on-site electron repulsion  $U$ , the dimerization strength  $\delta$  and the electronic localization is a crucial problem for second order phase transitions that requires the treatment of the infinite system within a correlated model. The problem is further complicated by the difficulties in determining the numerical values of the repulsion integrals  $U$ . Indeed, these quantities are difficult to obtain from ab-initio calculations on fragments, since they should take into account, in an effective way, the effects of the long-range electron repulsions, whenever those are not explicitly treated in the model. This problem is well known since the 50's by users of semi-empirical methods and an illustrative example is the drop of the effective Hubbard on-site  $\pi$ -repulsion of carbon atoms in conjugated molecules from 11eV for the benzene<sup>19</sup> to 6eV for polyenes<sup>20</sup>. An experimental evaluation of the repulsion  $U$  is possible from the activation energies of insulating or semiconducting compounds. However this would require precise theoretical evaluations of the charge gaps (ionization potential minus electro-affinity) as a function of  $U$  and the structural parameters.

The physical properties of these charge transfer salts can be modeled within the Hubbard<sup>21</sup> or  $t - J$ <sup>22</sup> formalisms reduced to the conduction band. The resolution of even such simple Hamiltonians requires a method able to deal with infinite systems. The Density Matrix Renormalization Group (DMRG) method<sup>23</sup> provides such a procedure for one-dimensional problems. The aim of the present work will be to modelize acceptor-based one-dimensional charge transfer salts such as the isostructural systems  $[Ni(dmit)_2]_2NR_4$  where  $NR_4 = NMe_4, NHMe_3, NH_2Me_2 \dots$ <sup>24</sup>. We will study a quarter-filled dimerized chain as a function of both the on-site repulsion  $U$  and the dimerization factor  $\delta$ . We will compute charge gaps and bond orders of this system, within an effective,  $U$ -dependent,  $t - J$  model. Properties for donor-based 3/4-filled systems can easily be deduced by particle-hole symmetry. Since the  $NH_2Me_2 [Ni(dmit)_2]_2$  compound is a semiconductor<sup>24</sup> we will be able to estimate the value of  $U$  for the  $Ni(dmit)_2$  molecule involved in that type of infinite molecular crystal.

In the next section we describe the DMRG method as well as the model Hamiltonian. Section III reports and analyses the results. The last section will be devoted to conclusions and perspectives.

## II. MODEL AND METHOD

### A. The model

Single-band quarter-filled systems have an average occupation per site of only half an electron. Therefore, independently of the value of the on-site repulsion, it can be expected that the bivalent anion states associated to  $[Ni(dmit)_2]^{2-}$  sites are very weakly represented in the ground-state wave-function. In the non-correlated limit (where the weight of the dianionic states is known to be maximum) their contribution is only  $1/16 = 0.0625$ . It is therefore reasonable to eliminate explicit reference to the di-anions in the effective model and to allow only the neutral state

$|0\rangle$  (no electron on the LUMO), and the two singly anionic states  $|\uparrow\rangle$  and  $|\downarrow\rangle$  (one electron on the LUMO) as accessible Valence-Bond states on each site. An often encountered confusion should however be clarified : the absence of the di-anions in the wave-function is not synonymous of an infinite on-site repulsion, as usually assumed by extension from the half-filled band case, but is only the consequence of their low statistical weight in a weakly-filled band system. In this case, the main physical effect of the bivalent anion molecular states is to lower the effective energy of the local singlets with respect to the local triplets. This is taken into account within a  $t - J$  Hamiltonian, where the role of the  $J$  exchange integral provides this effect.

$$\begin{aligned} H_{t-J} &= t \sum_{\langle i,j \rangle} \sum_{\sigma} \left( a_{i,\sigma}^{\dagger} a_{j,\sigma} + a_{j,\sigma}^{\dagger} a_{i,\sigma} \right) - J \sum_{\langle i,j \rangle} (a_{i,\uparrow}^{\dagger} a_{j,\downarrow}^{\dagger} - a_{i,\downarrow}^{\dagger} a_{j,\uparrow}^{\dagger}) (a_{i,\uparrow} a_{j,\downarrow} - a_{i,\downarrow} a_{j,\uparrow}) \quad (1) \\ &= t \sum_{\langle i,j \rangle} \sum_{\sigma} \left( a_{i,\sigma}^{\dagger} a_{j,\sigma} + a_{j,\sigma}^{\dagger} a_{i,\sigma} \right) + 2J \sum_{\langle i,j \rangle} \vec{S}_i \vec{S}_j - J/2 \end{aligned}$$

where  $a_{i,\sigma}^{\dagger}$  (resp.  $a_{i,\sigma}$ ) is the creation (resp. annihilation) operator of an electron of spin  $\sigma$  on the molecule  $i$ , so that  $a_{i,\uparrow}^{\dagger} a_{j,\downarrow}^{\dagger} - a_{i,\downarrow}^{\dagger} a_{j,\uparrow}^{\dagger}$  (resp.  $a_{i,\uparrow} a_{j,\downarrow} - a_{i,\downarrow} a_{j,\uparrow}$ ) is the creation (resp. annihilation) operator of a local singlet on the bond  $\langle i, j \rangle$ .  $t$  refers to the hopping integral between adjacent ( $\langle i, j \rangle$ ) molecules  $i$  and  $j$  while  $J$  is the effective exchange between them.

### 1. The effective exchange integral

There are different possible ways to extract the value of the effective  $J$  as a function of the hopping and repulsion integrals. We choose to extract it in a way such as to reproduce the spectroscopy of a dimer in the Hubbard models. This choice is motivated by the fact that the model should be valid over the whole range of  $U/|t|$ , which excludes all perturbative techniques. The ground-state of the Hubbard Hamiltonian on a dimer is a symmetric singlet  $^1\Sigma_g$  :

$$^1\Sigma_g = \cos \theta \frac{|\bar{i}\bar{j}\rangle - |\bar{i}j\rangle}{\sqrt{2}} + \sin \theta \frac{|\bar{i}\bar{i}\rangle + |\bar{j}\bar{j}\rangle}{\sqrt{2}} \quad (2)$$

$$\text{of energy } E_{hub}(^1\Sigma_g) = \frac{U - \sqrt{U^2 + 16t^2}}{2}$$

while the first excited state is a triplet  $^3\Sigma_g$  of energy 0. Within the  $t - J$  model the first excited state is similarly a triplet of energy 0 and the ground-state a symmetric singlet associated to the energy  $-2J$ . The equation of the low energy spectrum in the two formulations yields immediately

$$J = \frac{U - \sqrt{U^2 + 16t^2}}{4} \quad (3)$$

Let us notice that the effective exchange integral is a function of the correlation ratio  $U/|t|$ , going from  $t$  in the uncorrelated limit to  $-2t^2/U$  in the strongly correlated one. Even though  $J$  is extracted from the spectroscopy of a dimer, the validity of this model on infinite chains has been extensively studied in a previous work<sup>25</sup>.

## 2. The correlated effective bond order operator

It is clear that the elimination of the explicit reference to the di-anions in the wavefunction will obviously affect the values of any observable one may be interested in. One must therefore derive (as done above for the  $J$ ) effective observable operators in order to take into account the effects of these states.

In this paper we are more specifically interested in the bond order. It is easy to see that the bond order (over the  $\langle i, j \rangle$  bond) has a diagonal matrix in the above  $^1\Sigma_g$ ,  $^3\Sigma_g$  basis set and that its value for the triplet is strictly zero, both in the Hubbard and  $t - J$  models. The value of the ground-state bond order in the Hubbard model is

$$p_{hub}(^1\Sigma_g) = \sin 2\theta = \frac{4|t|}{\sqrt{U^2 + 16t^2}} = \frac{2tJ}{t^2 + J^2} \quad (4)$$

where  $\theta$  is defined in equation 2. This value will be assign to the singlet ground-state in the  $t - J$  representation. It comes an effective bond order operator

$$\begin{aligned} \hat{p} = & \frac{1}{2} \sum_{\langle i, j \rangle} \sum_{\sigma} \left( a_{i, \sigma}^{\dagger} a_{j, \sigma} + a_{j, \sigma}^{\dagger} a_{i, \sigma} \right) \\ & + \frac{tJ}{t^2 + J^2} \sum_{\langle i, j \rangle} (a_{i, \uparrow}^{\dagger} a_{j, \downarrow}^{\dagger} - a_{i, \downarrow}^{\dagger} a_{j, \uparrow}^{\dagger}) (a_{i, \uparrow} a_{j, \downarrow} - a_{i, \downarrow} a_{j, \uparrow}) \end{aligned}$$

## B. The DMRG method

The DMRG is a very powerful method proposed by S. White<sup>23</sup> a few years ago for the treatment of one dimensional spin systems. Since then it has become one of the leading numerical tools for the study of quasi-1D correlated quantum systems. This success is due to both its excellent accuracy for systems as large as a few hundred of sites, and its flexibility in terms of the model (Heisenberg,  $t - J$ , Hubbard, Kondo, etc).

In the DMRG approach the properties of the infinite system are derived by extrapolating the results of a succession of calculations on finite systems. Each one of these finite-system calculations is considered as a renormalization group (RG) iteration. The length  $N_{site}$  of the chain increases very slowly at each iteration. For instance, in the present case,  $N_{site}$  is increased by 2 sites (see Fig. 1). In spite of the fact that  $N_{site}$  increases, the dimension of the many-body Hilbert space is kept constant by means of the following procedure illustrated Fig. 1.

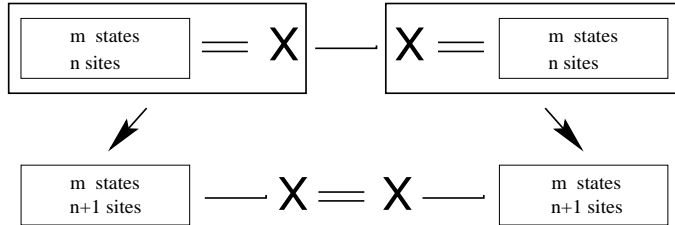


FIG. 1. Illustration of the renormalization procedure. A cross represents a  $Ni(dmit)_2$  molecule or  $t - J$  site. Single (resp. double) lines represent weak (resp. strong) interactions.

At each RG iteration the system is divided in two side blocks spanned by  $m$  local states (typically,  $m = 60, 82$  and  $100$  in the present calculations) and two central sites which require  $m_1$  local states, each to be represented exactly (e.g.,  $m_1 = 4$  for a Hubbard model and  $m_1 = 3$  for a  $t - J$  one). The Hilbert space for the  $N^{th}$  iteration (i.e. for the  $N_{site} = 2N + 2$  system) is obtained as the set of the antisymmetrized direct products of the four-blocks local states

$$\Phi_{ijkl} = |\phi_i^1 \otimes \phi_j^2 \otimes \phi_k^3 \otimes \phi_l^4\rangle$$

where  $\phi_i^b$  is the  $i^{th}$  local state of the block  $b$ . Thus the size of the Hilbert space is kept as  $(m \times m_1)^2$  all along the renormalization scheme.

Five main steps are involved in going from iteration  $N$  to iteration  $N + 1$ :

1. the ground state of the  $N_{site} = 2N + 2$  system is obtained using a full configurations interaction procedure,
2. the reduced ground-state density matrix of the superblock formed by one of the side blocks and its neighboring site is calculated (see Fig. 1),
3. the reduced density matrix is diagonalized and the eigenvectors yielding the  $m$  largest eigenvalues (i.e., occupations) are obtained,
4. the superblock local states space of size  $m \times m_1$  is projected onto the  $m$  most populated states derived in the previous step; the renormalized interactions within these superblocks, and between them and the central sites, are obtained by performing the corresponding unitary transformations,
5. the resulting Hamiltonian is then used for calculating the ground-state at the following iteration, i.e., we return to the first step until convergence is achieved.

The number of RG iterations performed in this work is 100, that is 202 effective  $Ni(dmit)_2$  molecules in the chain. The number of block states kept is 60, 82 and 100. The infinite system properties are then extrapolated from those of the finite (but large) systems.

### III. RESULTS AND DISCUSSION

The  $Ni(dmit)_2$ -based systems do not present structural dimerizations. However, molecular extended Hückel (EHT) calculations exhibit electronic dimerizations through alternated hopping integrals along the chain<sup>24</sup>. The recent reasonable description of the transport properties of the  $NH_2Me_2[Ni(dmit)_2]_2$  and the  $NHMe_3[Ni(dmit)_2]_2$  systems by Fermi surface EHT calculations<sup>24</sup> has proved the good quality of the calculated electronic dimerization ratio  $\delta = (t_c - t_l)/t_c$  where  $t_c$  refers to the *intra*-dimer hopping integral and  $t_l$  to the *inter*-dimer one.  $\delta = 0$  and  $\delta = 1$  correspond respectively to the non-dimerized and to the product of dimers limits. As announced previously, we computed the charge gap  $\Delta_c$ , that is the extrapolated difference (toward the infinite system limit) between the ionization potential and the electron affinity as a function of both  $U/|t_c|$  and  $\delta$ . If  $E(N_{site}, N_e)$  is the energy of a finite  $N_{site}$  sites system with  $N_e$  electrons :

$$\begin{aligned} \Delta_c &= \lim_{N_{site} \rightarrow \infty} \Delta_c(N_{site}) \\ &= \lim_{N_{site} \rightarrow \infty} \{E(N_{site}; N_{site}/2 + 1) + E(N_{site}; N_{site}/2 - 1) - 2 * E(N_{site}; N_{site}/2)\} \end{aligned}$$

.  $U/|t_c|$  spans the whole range of correlation strength between 0 and  $+\infty$ , while  $\delta$  is varied between the two extreme values given by the real systems, that is  $\delta = 0.05$  for the metallic phase  $NHMe_3[Ni(dmit)_2]_2$  and  $\delta = 0.75$  for the semiconducting one  $NH_2Me_2[Ni(dmit)_2]_2$ . In addition to the macroscopic picture given by the charge gap, we aimed to have a closer, microscopic understanding of the ground-state wave-function and of its localized versus delocalized character, that cannot be provided by extended Hückel calculations. These properties can be traced using the chemical bonding on the dimers, and more specifically the ratio between long- and short-bond order parameters

$$\lambda = \frac{p_l}{p_c} = \lim_{N_{site} \rightarrow \infty} \frac{p_l(N_{Site})}{p_c(N_{Site})}$$

where  $p_c$  and  $p_l$  are respectively the short- and long-bond orders.  $\lambda$  is expected to vary from 0 for the product of dimers limit to 1 for the totally delocalized system.

Owing to the present renormalization scheme that increases the number of sites by only 2 at each iteration, one encounters two specificities.

- The number of electrons is increased by 1 at each renormalization iteration, the ground state being a singlet for odd iterations ( $N = 2p - 1$ ,  $4p$  sites and  $2p$  electrons) and a doublet for the even ones ( $N = 2p$ ,  $4p + 2$  sites and  $2p + 1$ ) electrons. As a consequence all computed observables present an even-odd iterations alternation, requiring to compute separately the odd and even iterations limits — even though they both should converge to the same value.
- In order to keep a physically meaninfull system, one must impose the edge bonds to be consistently short. Thus, depending on the parity of the iteration, this leads to a long/short alternation of the central bond, on which the bond orders are computed.

Three series of calculations have been performed for  $m = 60$ , 82, and 100 block states kept. Let us notice that the  $m = 82$ , and 100 calculations treat exactly the finite systems up to 10 sites while the  $m = 60$  only treats them exactly up to 8 sites.

### A. Charge Gap

Figures 2a-b present the  $\delta$  dependence of the charge gap for 8 equidistant  $U/(U + 4t_c)$  values in the range  $[0, 1]$ . They correspond respectively to  $m = 60$  and  $m = 100$  block states kept at each iteration. The results for  $m = 82$  states have not been presented here since they are not qualitatively — and even quantitatively — much different from those obtained with  $m = 100$ .

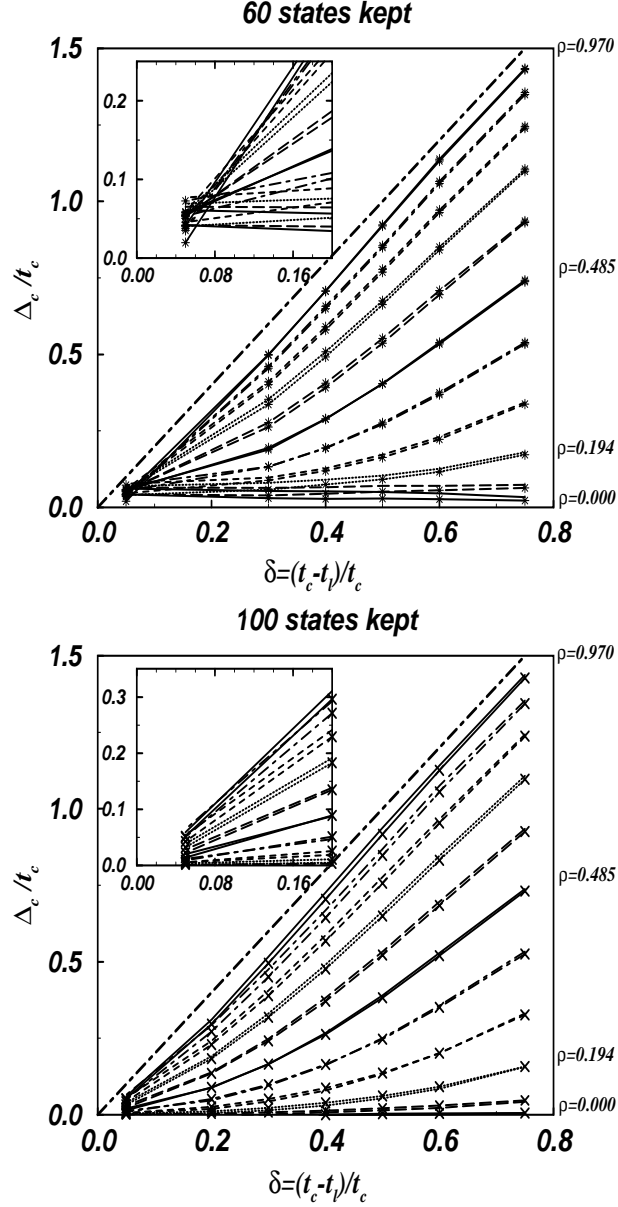


FIG. 2. Charge gaps in  $t_c$  units as a function of the dimerization factor  $\delta$ . Each curve corresponds to a different value of  $J/t$ , therefore of  $\rho = U/(U + 4t_c)$  which varies between 0 and 0.97 by step of 0.097. (a)  $m = 60$  and (b)  $m = 100$  block-states are kept.

While the two figures exhibit quite similar results for large dimerizations and large  $U$ , they differ substantially when either  $U$  or  $\delta$  are small. Indeed, in these latter regions, the  $m = 60$  calculations largely overestimate the values of the gaps compared to the ones obtained with  $m = 100$ . In the large dimerization region —  $\delta > 0.5$  — the increasing character of the gap as a function of the correlation strength  $U$  is well reproduced, even though the discrepancy with the  $m = 100$  curves increases rapidly when  $U$  decreases. In the small dimerization limit however, the  $m = 60$  results do not even exhibit the correct behavior as a function of  $U$ . Indeed, for  $\delta = 0.05$ , the smallest computed gap corresponds to the largest value of  $U$  (the extrapolated gap for  $U = 0$  and  $\delta = 0$  is 0.05 instead of 0). Moreover,

unphysical crossings between  $U$ -curves can be observed. Those artefactual effects can be directly related to an insufficient number of block states kept in the  $m = 60$  calculations, since they disappear when  $m$  is increased to 82 or 100. This larger  $m$  value required for an adequate treatment in the small  $\delta$  and/or small  $U$  region can be rationalized in the following way.

- The populations of the local block states in the total wave-function are known<sup>26</sup> to follow a decreasing exponential of the form  $\gamma = \exp(-\alpha(U)n)$ , where  $\alpha(U)$  is a decreasing function of  $U$ . As documented in ref<sup>26</sup>, the accuracy of a DMRG calculation is directly related to the fraction of the total population provided by the  $m$  block-states kept. Hence, as  $U$  decreases, a larger number of states  $m$  needs to be kept.
- An optimal use of the DMRG procedure supposes that the perturbation imposed on the electronic wave-function follows a linear dependence with the system size. In the present case, the addition or removal of an electron is a major perturbation for small size systems (50% of the electronic population in the first iteration for the  $N_{site}/2 - 1$  system) whereas it is a negligible one for larger systems (100/( $N + 1$ )% at the  $N^{\text{th}}$  iteration). This problem can only be overcome by insuring that all local states needed for the description of the large systems (weakly perturbed) are not removed in the first few iterations. That is by increasing the size of the largest system treated exactly and equivalently enlarging  $m$  (8 sites for  $m = 60$ , 10 sites for  $m = 82$  or  $m = 100$ ).

From now we will focus our attention on the  $m = 100$  results.

As expected the charge gap is an increasing function of both the dimerization ratio and the on-site repulsion. In agreement with the quarter-filled dimerized Hückel model, the  $U = 0$  curve does not exhibit any significant gap. Its maximum computed value is  $0.005|t_c|$  and can be considered as characteristic of the calculations precision. Similarly, all curves extrapolate towards a zero gap for  $\delta = 0$ .

In large  $U$  limit the exchange  $J$  parameter tends to 0 ; the infinite- $U$  Hamiltonian is therefore limited to the kinetic part acting on a Hilbert space excluding all doubly occupied sites.

$$H_{U \rightarrow +\infty} = \sum_{\langle i,j \rangle} \sum_{\sigma} \left( a_{i\sigma}^{\dagger} a_{j\sigma} + a_{j\sigma}^{\dagger} a_{i\sigma} \right)$$

The spin part of the latter Hamiltonian is completely uncoupled from the space part and the system is equivalent to a spinless fermion one. As shown in ref.<sup>27</sup> the ground-state energy per site can be expressed as

$$E = t_c \frac{2 - \delta}{\pi} E \left( \phi, 2 \frac{\sqrt{1 - \delta}}{2 - \delta} \right)$$

where

$$\phi = \begin{cases} \pi n & \text{for } n > 1/2 \\ \pi(1 - n) & \text{for } n < 1/2 \end{cases}$$

$n$  refers to the band filling,  $E$  to the elliptic integrals of the second kind. One sees immediatly that the energy derivative presents a discontinuity as a function of the band-filling, discontinuity that can be associated to the charge gap.

$$\frac{\Delta_c}{t_c} = \frac{2 - \delta}{\pi} 2\pi \sqrt{1 - \left( 2 \frac{\sqrt{1 - \delta}}{2 - \delta} \right)^2} = 2\delta$$



Turning back our attention to fig. 2b one sees that our calculations converge well to the above expected limit for  $U \rightarrow +\infty$ .

One of the main interest of having an accurate estimate of the charge gap within a correlated model is the ability it provides to evaluate the effective repulsion  $U$ . Organic conductors are well-known to behave as strongly correlated systems, since the rather weak inter-molecular interactions lead to quite large  $U/|t|$  ratio. However the difficulties encountered to obtain reliable  $U$  has led to very large controversies for years<sup>28</sup>. On one hand, a non biased extraction from experimental datas would require the use of a correlated interpretative model beyond the standard non or weakly correlated methods (Hückel, RPA<sup>29</sup>). On another hand, direct computation from ab initio quantum chemistry methods on the molecular unit is expected to (largely) overestimate the value of  $U$ . As already mentionned in the introduction, the  $U$  integral is an effective integral that takes into account number of other correlation effects than the purely one-site repulsion.

The availability of accurate gap values within a correlated model, valid over the whole  $U/|t_c|$  range, allows us to confront them to the experimental activation energies in order to extract reliable values of  $U$ . Single-crystal temperature-dependent conductivity measurements have disclosed an activation energy of  $E_a = 0.21\text{eV}$ <sup>24</sup>, at room temperature, for the semiconductor  $NH_2Me_2 [Ni(dmit)_2]_2$ . Considering that at room temperature the gap is reduced by the thermal energy, the  $k_bT$  value should be added to  $E_a$  in order to obtain its  $T = 0$  estimation. One therefore obtains an estimated experimental gap at  $T = 0K$  of  $E_a(0K) = 0.22\text{eV}$ , that is  $E_a(0K) = 0.76|t_c|$  (where  $t_c = 0.29\text{eV}$  has been taken from EHT calculations<sup>24</sup>). This corresponds to  $U = 4.0|t_c| = 1.16\text{eV}$  for  $\delta = 0.75$ . Following the same line of argument for the  $NHMe_3 [Ni(dmit)_2]_2$  compound, the  $\frac{1}{2}k_bT$  factor appears to be larger than the computed gap for the whole range of  $U/|t_c|$ . Although the calculated gap  $\Delta_c$  never equals zero, the small values it takes are in agreement with the metallic behavior exhibited by this system. Using now the value of  $U$  obtained for the  $Ni(dmit)_2$  molecule and the EHT  $t_c = 0.237\text{eV}$  value for the  $NHMe_3 [Ni(dmit)_2]_2$  system, the correlation ratio comes to be  $U = 4.89|t_c|$ , slightly larger than for the semiconducting phase.

## B. Bond Order

Fig. 3 reports the short- and long-bond orders (respectively referenced as  $p_c$  and  $p_l$ ) as a function of  $U/|t_c|$  and for different dimerizations.  $p_c$  and  $p_l$  have been computed according to the expression derived in section II A 2, i.e. the effects of the di-anionic configurations are taken into account in an effective way. From a technical point of view, the bond order was computed on the central bond at each iteration. In the present renormalization scheme, this bond alternates from long for odd iterations, to short for even iterations. Additional oscillations occur between  $(4p)$ - and  $(4p+2)$ -electrons systems for long bonds and  $(4p+1)$ - and  $(4p+3)$ -electrons systems for short bonds. We therefore performed 4 independent extrapolations. For short bonds, the  $(4p+1)$ - and  $(4p+3)$ -electrons extrapolations converge towards the same values all over the  $U/|t_c|$  range. However, as can be seen on Fig. 3, for long bonds, the  $(4p+2)$ - and  $(4p)$ -electrons extrapolated  $p_l$  curves split over for small  $U$ , following the aromatic, anti-aromatic alternation<sup>30</sup>.

As expected, when the dimerization factor goes to 1, the system tends toward a product of independent singly-occupied dimers, that is  $p_c$  tends to 0.5 and  $p_l$  to 0. Looking now at the  $U = 0$  and  $U \rightarrow +\infty$  limits, one can perform an analytical calculation as a function of  $\delta$ . It is easy to reach the Hückel result

$$p_c(\delta) = \frac{1}{\pi} \int_0^{\pi/2} \frac{1 + (1 - \delta) \cos \theta}{\sqrt{1 + (1 - \delta)^2 + 2(1 - \delta) \cos \theta}} d\theta \quad (5)$$

The  $U \rightarrow +\infty$  result can be obtained from the spinless fermion case as treated in ref.<sup>27</sup>, and

$$\begin{aligned} p_c(\delta) &= \langle c_0^\dagger c_1 \rangle \\ &= \frac{1}{2\pi} [\delta F(1/2, q) + (2 - \delta) E(1/2, q)] \end{aligned} \quad (6)$$

where

$$\begin{aligned} E(1/2, q) &= \int_0^{\pi/2} \frac{1}{\sqrt{1 - 4q \sin^2 \theta}} d\theta \\ E(1/2, q) &= \int_0^{\pi/2} \sqrt{1 - 4q \sin^2 \theta} d\theta \\ q &= \frac{1 - \delta}{(2 - \delta)^2} \end{aligned}$$

The asymptotic values are represented by open circles in Fig. 3, all of them in very good agreement with our computed curves.

According to the dimerization factor  $\delta$ , the different systems studied in fig. 3 present two types of behavior. The first type, which will be referred as *localized*, includes the  $\delta = 0.5$  and  $\delta = 0.75$  ( $NH_2Me_2 [Ni(dmit)_2]_2$ ) systems. It is characterized not only by a small  $p_l/p_c$  ratio (as seen in Fig. 4) but also by a non monotonic behavior of the short-bond order as a function of  $U/|t_c|$ . Starting from the Hückel limit,  $p_c$  begins to decrease, goes through a minimum ( $p_c^{min}(\delta)$ ), then increases up to a  $U \rightarrow +\infty$  limit, slightly smaller than the  $U = 0$  one. The  $U/|t_c|$  value associated to  $p_c^{min}(\delta)$  is a decreasing function of  $\delta$ . The second type of behavior, to which we will refer as *delocalized*, is represented by the  $\delta = 0.05$  ( $NHMe_3 [Ni(dmit)_2]_2$ ) system. It is characterized by a  $p_l/p_c$  ratio close to 1 and a monotonically decreasing  $p_c$  curve as  $U/|t_c|$  increases. The  $\delta = 0.2$   $p_c$  curve however exhibit an intermediate behavior between the two previous ones,  $p_c$  first decreases as  $U$  increases, then reaches an asymptotic value around  $U = 4|t_c|$ .

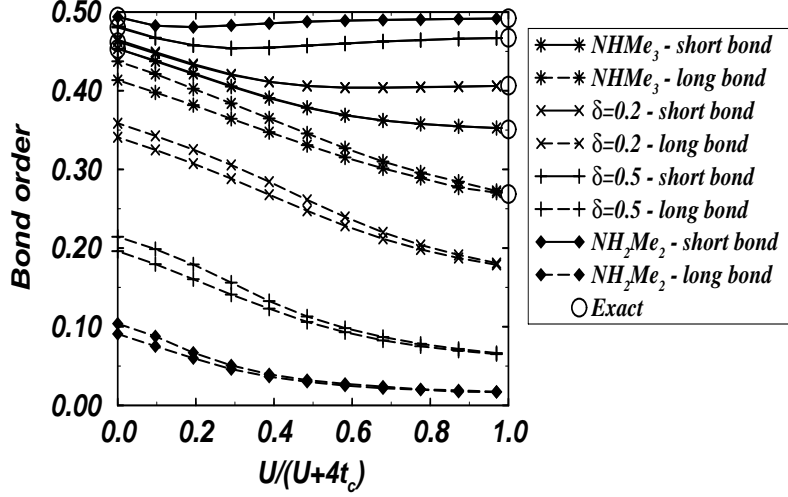


FIG. 3. Long- and short-bond orders as a function of  $U/(U+4t_c)$ . Solid line: short-bond order, dashed line: long-bond order. The circles correspond to analytical evaluations of the asymptotic values for  $U = 0$  and  $U \rightarrow \infty$ .

The long-bond order presents a qualitatively (but not quantitatively) similar behavior for all dimerization values, decreasing as the correlation strength raises and exhibiting an inflexion point. The latter occurs for smaller  $U/|t_c|$  values as  $\delta$  increases. As expected the long-bond order diminishes as  $\delta$  increases, while the reverse tendency is observed for the short-bond order.

Figure 4 presents the  $p_l/p_c$  ratio as a function of the correlation strength. It can be seen in this figure that — as expected — the correlation has a localizing effect since  $p_l/p_c$  diminishes as  $U/|t_c|$  increases for all values of  $\delta$ . It is more interesting to compare the hopping-integral ratio (horizontal lines) to the bond-order one. The *delocalized* system exhibits similar  $t_l/t_c$  and  $p_l/p_c$  ratios. On the contrary, the *localized* systems show much smaller long- to short-bond order ratios than the hopping-integrals do, i.e. the collective effects seem to strongly enhance the localization of the electron density on the dimers.

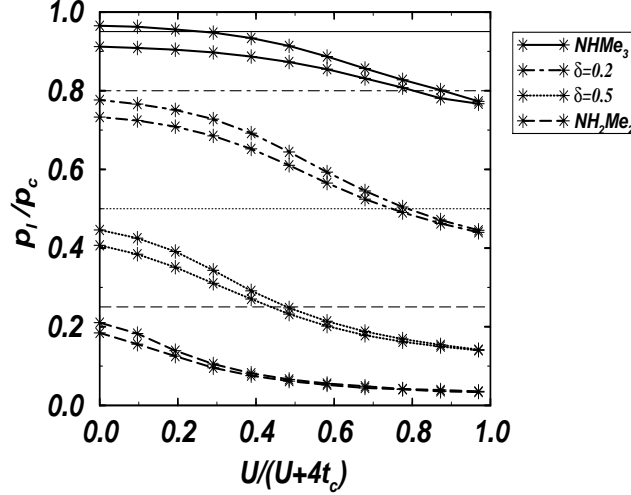


FIG. 4. Bond-orders ratio:  $p_l/p_c$ . Solid line:  $\delta = 0.05$ , dash-dotted line:  $\delta = 0.20$ , dotted line:  $\delta = 0.50$ , long-dashed line:  $\delta = 0.75$ .

#### IV. CONCLUSION

The present work deals with the correlation and dimerization effects in quarter-filled quasi one-dimensional organic conductors such as the  $X [M(dmit)_2]_2$  radical anions compounds (where  $M$  stands for  $Ni$ ,  $Pt$  or  $Pd$ ). We treated them as a correlated dimerized chain within a  $t - J$  model. The effective exchange integral  $J$  is taken as a function of the hopping integral  $t$  and the correlation strength  $U$ , derived to reproduce the dimer low energy spectroscopy. We computed accurately the charge gaps for the infinite chain (using the DMRG method) over the whole range of electronic repulsion and dimerization factor. The comparison between our theoretical results and the experimental activation energy on semiconducting  $Ni(dmit)_2$ -based compounds allowed us to extract a reasonable evaluation of the one-site repulsion integral  $U$  for the  $Ni(dmit)_2$  molecule:  $1.16eV$ , i.e.  $U/|t_c| = 4.0$  for the semiconducting  $NH_2Me_2 [Ni(dmit)_2]_2$  compound, and  $U/|t_c| = 4.89$  for the metallic  $NHMe_3 [Ni(dmit)_2]_2$  one. It would be interesting to extract, in the same way, the  $U/|t|$  value for other molecules widely encountered in such molecular compounds, specifically since there is a large number of controversies about their numerical values.

We also computed the long and short bond order as a function of both  $\delta$  and  $U$  and showed that the collective effects enhance, in strongly dimerized systems, the electronic localization on the dimer units. Meanwhile an unexpected  $U/|t_c|$  behavior has been found for these dimerized systems, with the observation of a minimum on the short-bond order curves. The increase of  $p_c$  for large  $U$  supports the idea that the electron repulsion enhances the accumulation of electrons on the strong dimers, leading to a product of dimer zeroth-order picture even for moderately dimerized systems ( $\delta = 0.5$ ).

- <sup>1</sup> K. Bechgaard, C. S. Jacobsen, K. Mortensen, M. J. Pedersen, N. Thorup Solid State Com. **33** 1119 (1980) ; K. Bechgaard, K. Carneiro, F. G. Rasmussen, K. Olsen, G. Rindorf, C. S. Jacobsen, H. J. Pederson, J. E. Scott, J. Am. Chem. Soc. **103** 2440 (1981) ; D. Jérôme, A. Mazaud, M. Ribault, K. Bechgaard, J. Phys. Lett. **41** L95 (1980).
- <sup>2</sup> J. M. Williams, A. J. Schultz, U. Geiser, K. D. Carlson, A. M. Kini, H. H. Wang, W. K. Kwok, M.-H. Whangbo, J. E. Schirber, Science **252** 1501 (1991) ; J. R. Ferraro, J. M. Williams, "Introduction to Synthetic Electrical Conductors", Academic Press., Orlando, FL (1987) ; T. Ishiguro, K. Yamaji, "Organic Superconductors", Springer-Verlag, Heidelberg Germany (1990).
- <sup>3</sup> For a review see : L. P. Gork'ov and G. Grner eds., "Charge Density Waves in Solids", North Holland (1989).
- <sup>4</sup> R. E. Peierls, "Quantum Theory of Solids", Oxford University Press (1955).
- <sup>5</sup> A. Andrieux, D. Jérôme, K. Bechgaard, J. Phys. Lett. **42** L87 (1981) ; J. C. Scott, H. J. Pedersen, K. Bechgaard, Phys. Rev. B **24** 475 (1981).
- <sup>6</sup> N. F. Mott, "Metal-Insulator Transitions", London : Taylor and Francis (1974).
- <sup>7</sup> M.-L. Doublet, E. Canadell, R. P. Shibaeva, J. Phys. France I **4** 1479, (1994).
- <sup>8</sup> M. M. Labes, P. Love, L. F. Nichols, Chem. Rev. **79** 1 (1979) ; D. Jérôme, H. J. Schulz, Adv. Phys. **31** 299 (1982).
- <sup>9</sup> For a review see : J. Wosnitza, Int. J. Modern Phys. B **7** 2707 (1993) ; J. Wosnitza, "Fermi Surfaces of Low-Dimensional Organic Metals and Superconductors", Springer-Verlag, Berlin (1997).
- <sup>10</sup> M.-H. Whangbo, "Crystal Chemistry and Properties of Materials with Quasi-One-Dimensional Structures", ed. J. Rouxel, Reidel : Dordrecht 27 (1986).
- <sup>11</sup> J. D. Martin, M.-L. Doublet, E. Canadell, J. Phys. France I **3** 2451 (1993).
- <sup>12</sup> M.-H. Whangbo, J. Ren, W. Liang, E. Canadell, J.-P. Pouget, S. Ravy, J. M. Williams, Solid State Com. **31** 4169 (1992).
- <sup>13</sup> For a review see : P. Fulde, "Electron Correlation in Molecules and Solids", Springer-Verlag, Berlin (1995).
- <sup>14</sup> V. E. Kampar, Russian Chem. Rev. **51** 185 (1982) ; M. L. Khidekel, E. I. Zhilyaeva, Synth. Met. **4** 1 (1981) ; R. N. Lyubovskaya Russian, Chem. Rev. **52** 736 (1983) ; M. Mizuno, A. F. Garito, M. P. Cava, J. Chem. Soc. Chem. Comm. 18 (1978).
- <sup>15</sup> G. Steimecke, R. Kirmse, E. Z. Hoyer ; P. Cassoux, L. Valade, H. Kobayashi, A. Kobayashi, R. A. Clark, A. E. Underhill, Coord. Chem. Rev. **110** 115 (1991).
- <sup>16</sup> R. Kato, H. Kobayashi, A. Kobayashi, T. Naito, M. Tamura, H. Tajima, H. Kudora, Chem. Lett. 1839 (1989) ; B. Garreau, B. Pomarède, C. Faulmann, J.-M. Fabre, P. Cassoux, J.-P. Legors, C. R. Acad. Sci. Paris **III-313** 509 (1991).
- <sup>17</sup> M.-H. Whangbo, R. Hoffmann, J. Am. Chem. Soc. **100** 6093 (1978).
- <sup>18</sup> R. J. Hoffmann, J. Chem. Phys. **39** 1397 (1963).
- <sup>19</sup> R.G. Parr, "The quantum theory of molecular electronicstructure", Benjamin, New-York (1963).
- <sup>20</sup> A.L. Tchougreeff and R. Hoffmann, J. Phys. Chem. **22** 96 (1992).
- <sup>21</sup> J. Hubbard, Proc. R. Soc. **276** 238 (1963).
- <sup>22</sup> E. Dagoto, Rev. Mod. Phys. **66** 104 (1991).
- <sup>23</sup> S. R. White, Phys. Rev. Lett. **69** 2863 (1992) ; S. R. White, Phys. Rev. B **48** 10345 (1993).
- <sup>24</sup> B. Pomarède, B. Garreau, I. Malfant, L. Valade, P. Cassoux, J.-P. Legros, A. Audouard, L. Brossard, J.-P. Ulmet, M.-L. Doublet, E. Canadell, Inorg. Chem. **33** 3401 (1994).
- <sup>25</sup> M.-B. Lepetit, M.-L. Doublet, to be published.
- <sup>26</sup> M.-B. Lepetit and G. M. Pastor, Phys. Rev. **B56**, 4447 (1997).
- <sup>27</sup> K. Penc and F. Mila, Phys. Rev. **B50** 11429 (1994).
- <sup>28</sup> F. Castet, A. Fritsch and L. Ducasse, J. Phys. France I, Condensed Matter **6** 583 (1996) ; D. Jerome, Solid State Comm. **92** 89 (1994)
- <sup>29</sup> F. Guinea, E. Louis, J. A. Vergés, Phys. Rev. B **45** 4752 (1992) ; F. Guinea, E. Louis, J. A. Vergés, Europhys. Lett. **17** 455 (1992).
- <sup>30</sup> T.E. Peacock, "Electronic Properties of Aromatic and Heterocyclic Molecules", A.P:

London (1965).